Antibiotic efficacy is linked to bacterial cellular respiration

Michael A. Lobritz[a,b,c,d,e,1,2], Peter Belenky[f,1], Caroline B. M. Porter[b,c], Arnaud Gutierrez[b,c], Jason H. Yang[b,c], Eric G. Schwarz[g], Daniel J. Dwyer[h], Ahmad S. Khalil[a,g,2], and James J. Collins[a,b,c,i,2]

[a]Wyss Institute for Biologically Inspired Engineering, Harvard University, Boston, MA 02115; [b]Institute for Medical Engineering & Science, Department of Biological Engineering, and Synthetic Biology Center, Massachusetts Institute of Technology, Cambridge, MA 02139; [c]Broad Institute of MIT and Harvard, Cambridge, MA 02139; [d]Division of Infectious Diseases, Massachusetts General Hospital, Boston, MA 02114; [e]Harvard Medical School, Boston, MA 02115; [f]Department of Molecular Microbiology and Immunology, Brown University, Providence, RI 02912; [g]Department of Biomedical Engineering and Biological Design Center, Boston University, Boston, MA 02215; [h]Department of Cell Biology and Molecular Genetics, Institute for Physical Science and Technology, Department of Biomedical Engineering, and Maryland Pathogen Research Institute, University of Maryland, College Park, MD 20742; and [i]Harvard-MIT Program in Health Sciences and Technology, Cambridge, MA 02139

This contribution is part of the special series of Inaugural Articles by members of the National Academy of Sciences elected in 2014.

Contributed by James J. Collins, May 18, 2015 (sent for review November 22, 2014; reviewed by Bruce R. Levin and Evgeny A. Nudler)

Bacteriostatic and bactericidal antibiotic treatments result in two fundamentally different phenotypic outcomes—the inhibition of bacterial growth or, alternatively, cell death. Most antibiotics inhibit processes that are major consumers of cellular energy output, suggesting that antibiotic treatment may have important downstream consequences on bacterial metabolism. We hypothesized that the specific metabolic effects of bacteriostatic and bactericidal antibiotics contribute to their overall efficacy. We leveraged the opposing phenotypes of bacteriostatic and bactericidal drugs in combination to investigate their activity. Growth inhibition from bacteriostatic antibiotics was associated with suppressed cellular respiration whereas cell death from most bactericidal antibiotics was associated with accelerated respiration. In combination, suppression of cellular respiration by the bacteriostatic antibiotic was the dominant effect, blocking bactericidal killing. Global metabolic profiling of bacteriostatic antibiotic treatment revealed that accumulation of metabolites involved in specific drug target activity was linked to the buildup of energy metabolites that feed the electron transport chain. Inhibition of cellular respiration by knockout of the cytochrome oxidases was sufficient to attenuate bactericidal lethality whereas acceleration of basal respiration by genetically uncoupling ATP synthesis from electron transport resulted in potentiation of the killing effect of bactericidal antibiotics. This work identifies a link between antibiotic-induced cellular respiration and bactericidal lethality and demonstrates that bactericidal activity can be arrested by attenuated respiration and potentiated by accelerated respiration. Our data collectively show that antibiotics perturb the metabolic state of bacteria and that the metabolic state of bacteria impacts antibiotic efficacy.

E. coli | *S. aureus* | antibiotics | cellular respiration | metabolomics

Bacteriostatic antibiotics inhibit cell growth whereas bactericidal antibiotics induce cell death. Classifying an antibiotic as bacteriostatic or bactericidal is based on an operational in vitro test (1), which offers a limited perspective on the physiologic activity of the antibiotic. Although the clinical value of bactericidal activity in the treatment of infection is a point of debate (1, 2), evidence supports a preference for bactericidal antibiotics for certain high-risk infections (2–8). The use of antibiotic combinations to treat bacterial infections is increasingly common, but the predictability of this approach is limited (9, 10). It is well-known that bacteriostatic–bactericidal combination treatments result in attenuation of bactericidal activity in vitro across a range of drugs and organisms (11–18). Clinically, this effect can have negative consequences in high morbidity infections like meningitis (19, 20), or positive effects by inhibiting lysis and exotoxin release in toxin-mediated syndromes (21, 22). How bacteriostatic antibiotics can block bactericidal lethality, however, is not well-understood.

Recent lines of evidence have suggested that antibiotics induce cellular metabolic shifts as a secondary response to their target interaction. The generation of antagonistic metabolic responses may be one possible means by which bacteriostatic and bactericidal antibiotics interact. The predominant cellular process targeted by bacteriostatic antibiotics is translation, which is thought to account for a major portion of the energy consumption in the cell at steady state (23, 24). Consequently, disruption of this process may cause significant changes in cellular energy dynamics (25). In support of this notion, the proteomic response to the bacteriostatic antibiotic chlortetracycline involves downregulation of major metabolic pathways (26), potentially suggesting a reduction in metabolic rates. In comparison with the bacteriostatic response, evidence suggests that bactericidal agents may increase cellular metabolic rates and that bactericidal antibiotic efficacy may relate directly to metabolic state (27). The transcriptional response to bactericidal antibiotics involves upregulation of genes involved in central metabolism and respiration (28–30). Direct metabolomic profiling of *Mycobacterium tuberculosis*

Significance

The global burden of antibiotic resistance has created a demand to better understand the basic mechanisms of existing antibiotics. Of significant interest is how antibiotics may perturb bacterial metabolism, and how bacterial metabolism may influence antibiotic activity. Here, we study the interaction of bacteriostatic and bactericidal antibiotics, the two major phenotypic drug classes. Interestingly, the two classes differentially perturb bacterial cellular respiration, with major consequences for their intrinsic activity both alone and in combination. Of note, bacteriostatic antibiotics decelerate cellular respiration, generating a metabolic state that is prohibitive to killing. Further, we show that the efficacy of bactericidal drugs can be improved by increasing basal respiration, and we identify a respiration-related drug target that potentiates the activity of bactericidal antibiotics.

Author contributions: M.A.L., P.B., C.B.M.P., D.J.D., A.S.K., and J.J.C. designed research; M.A.L., P.B., C.B.M.P., A.G., J.H.Y., and E.G.S. performed research; M.A.L., P.B., C.B.M.P., A.G., J.H.Y., A.S.K., and J.J.C. analyzed data; and M.A.L., P.B., C.B.M.P., D.J.D., and J.J.C. wrote the paper.

Reviewers: B.R.L., Emory University; and E.A.N., New York University.

Conflict of interest statement: J.J.C. is a scientific cofounder and Scientific Advisory Board chair of EnBiotix, Inc., a start-up focused on antibiotic development.

Freely available online through the PNAS open access option.

See QnAs on page 8160.

[1]M.A.L. and P.B. contributed equally to this work.

[2]To whom correspondence may be addressed. Email: jimjc@mit.edu, mlobritz@mgh.harvard.edu, or akhalil@bu.edu.

This article contains supporting information online at www.pnas.org/lookup/suppl/doi:10.1073/pnas.1509743112/-/DCSupplemental.

treated with a range of bactericidal agents demonstrated commonalities in remodeling of central metabolism in response to therapy (31). With regard to cellular metabolic state, the efficacy of bactericidal antibiotic therapy has been linked to carbon flux through the TCA cycle (32, 33), and environmental factors that engage with central metabolism, such as the availability of molecular oxygen to feed the electron transport chain, have also been linked to cell killing by antibiotics (34, 35).

Previous work has indicated that the cellular response to bactericidal antibiotics leads to overflow metabolism and the formation of reactive oxygen species (ROS) as part of their lethality (29, 35, 36), suggesting that accelerated metabolism is a key component of bactericidal activity. Consistent with this hypothesis, we have previously identified divergent effects of bactericidal antibiotics and the bacteriostatic translation inhibitor chloramphenicol on cellular respiration in *Escherichia coli* (35). In the present study, we assess the long-known phenotype of bacteriostatic and bactericidal antibiotic antagonism to address how antibiotics perturb bacterial metabolism and how cellular metabolic state influences antibiotic efficacy. We find that perturbation of cellular respiration is a major byproduct of antibiotic–target interaction. Further, changes in basal rates of cellular respiration can specifically tune the efficacy of bactericidal antibiotics. We identify that bacteriostatic antibiotics generate a metabolic state in bacteria that is prohibitive to killing, which may relate directly to the clinical outcomes identified in combination therapy.

Results

Bacteriostatic Antibiotics Decelerate Cellular Respiration. To assess physiologic changes induced by bacteriostatic and bactericidal antibiotics at the level of cellular respiration, we used a recently described real-time prokaryotic respiration assay using the SeaHorse XF^e extracellular flux analyzer (35). This platform measures real-time oxygen consumption rate (OCR) at picomole resolution, which we use as a proxy of cellular respiration (37) (Fig. 1 and Fig. S1). The assay detects oxygen using a solid-state sensor probe in a fluid chamber above a bacterial cell monolayer; thus, oxygen does not need to additionally diffuse through the probe solution matrix. We optimized the assay performance for cell input (Fig. S1*A*) and validated that OCR is dependent upon the presence of metabolizable carbon sources (Fig. S1*B*). The assay performed in M9 medium (in *E. coli*) limits growth effects, results in linear increases in OCR over time (Fig. 1*A*), and does not require normalization (35). *Staphylococcus aureus* respiration in minimal media fell below the limit of detection, and thus we adapted the assay to a standard rich media [tryptic soy broth (TSB)], which demonstrated logarithmic increases in OCR (consistent with more rapid doubling rates) and required normalization using instantaneous live–dead staining (35) (Fig. 1*B*).

Treatment of *E. coli* with bacteriostatic translation inhibitors resulted in rapid deceleration of cellular respiration (Fig. 1*A*, *Left*). This effect was evident as early as 6 min after exposure to drug and was sustained (Fig. S1*C*). In contrast, three canonical bactericidal antibiotics [ampicillin (Amp), gentamicin (Gent), and norfloxacin (Nor)] accelerated respiration (Fig. 1*A*, *Right*) with varying kinetics. Rifampin (Rif), commonly considered bacteriostatic in *E. coli* and bactericidal in *S. aureus* (Fig. S2), potently suppressed OCR in *E. coli* (Fig. 1*A*, *Right*). Treatment of *S. aureus* with bacteriostatic translation inhibitors also resulted in rapid inhibition of OCR (Fig. 1*B*, *Upper Left*). OCR measurements from bactericidal treatment of *S. aureus* without normalization demonstrated distinct dynamics from bacteriostatic antibiotics (Fig. 1*B*, *Lower Left*). Normalization for instantaneous live cells yielded accelerated OCR by levofloxacin (Levo) but not daptomycin (Dapto) whereas normalization showed consistent deceleration from chloramphenicol (Cam) treatment (Fig. 1*B*, *Bottom Right*). Dapto treatment resulted in very high propidium iodide-positive cells, as expected, due to an increase in cell permeability as a major component of its activity (Fig. S1*D*). Rif treatment of *S. aureus*, which exhibits time-dependent killing rather than concentration-dependent killing (Fig. S2), rapidly suppressed OCR in a pattern

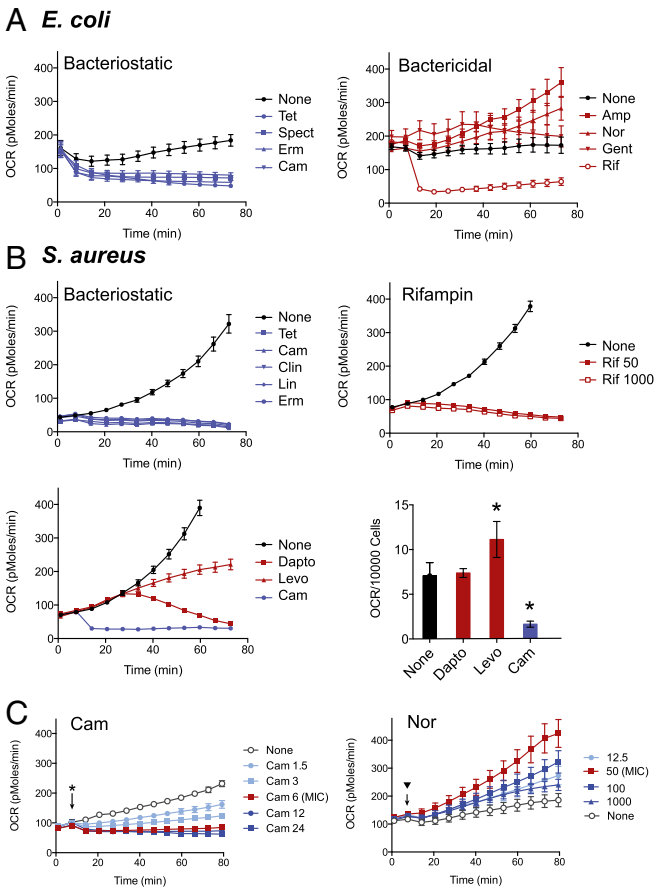

Fig. 1. Antibiotics perturb bacterial respiration. Real-time changes in oxygen consumption rate (OCR, in picomoles of molecular oxygen per minute) in response to antibiotic treatment in *E. coli* and *S. aureus* were measured on a Seahorse XF^e Extracellular Flux Analyzer. (*A*, *Left*) OCR of *E. coli* treated with the following bacteriostatic antibiotics (5× MIC): tetracycline (Tet), spectinomycin (Spect), erythromycin (Erm), or chloramphenicol (Cam), compared with media plus vehicle. (*Right*) Real-time OCR of *E. coli* treated with the bactericidal antibiotics ampicillin (Amp), norfloxacin (Nor), gentamicin (Gent), or rifampin (Rif) at 5× MIC. (*B*) Real-time OCR of *S. aureus* treated with tetracycline (Tet), chloramphenicol (Cam), clindamycin (Clin), linezolid (Lin), or erythromycin (Erm) compared with vehicle-treated cells in TSB at 5× MIC. (*Upper Right*) OCR response to rifampin (Rif) in *S. aureus* relative to vehicle treated control at 4× MIC (50 ng/mL) and 80× MIC (1,000 ng/mL). (*Lower Left*) Demonstrates OCR of *S. aureus* in response to Cam, daptomycin (Dapto), and levofloxacin (Levo). (*Lower Right*) Normalized OCR per live cell. (*C*) *E. coli* OCR measurement with a dose range of chloramphenicol (μg/mL, MIC = 6 μg/mL). (*Right*) *E. coli* OCR measurement with a dose range of norfloxacin (ng/mL, MIC = 50 ng/mL) over time. Data represent mean ± SEM of eight replicates. Where appropriate, statistical analysis is shown (*$P \leq 0.01$).

consistent with other bacteriostatic antibiotics (Fig. 1*B*, *Upper Right*). Thus, bacteriostatic translation inhibitors broadly decelerate cellular respiration whereas most bactericidal antibiotics accelerate respiration. Dapto had a neutral effect on respiration whereas Rif suppressed respiration in *S. aureus* despite killing.

We next explored respiration effects caused by antibiotics around the minimum inhibitory concentration (MIC). OCR was monitored in *E. coli* treated with Cam (MIC 6 μg/mL) from 1.5 μg /mL (1/4× MIC) to 24 μg/mL (4× MIC). Deceleration of OCR was maximally achieved at the MIC concentration (Fig. 1*C*), with no substantial changes by higher concentrations. Sub-MIC Cam resulted in dose-dependent inhibition of OCR (Fig. 1*C*). In comparison, treatment of *E. coli* with Nor from 12.5 ng/mL (1/4× MIC) to 1 μg/mL (20× MIC) demonstrated dynamic elevations in respiration with maximal acceleration of OCR observed

at the MIC (Fig. 1*C*). Interestingly, exposure to subinhibitory concentrations of Nor was sufficient to accelerate cellular respiration (Fig. 1*C*).

Respiration-Decelerating Antibiotics Block Lethality of Respiration-Accelerating Antibiotics. Having observed divergent effects on cellular respiration by bacteriostatic and bactericidal antibiotics, we next assessed the outcome of combination treatments on cell survival. We performed a pairwise lethality screen of 36 clinically relevant bacteriostatic-bactericidal antibiotic combinations in both *E. coli* (16 combinations) and *S. aureus* (20 combinations) by time-kill analysis (Fig. 2 and Fig. S3). We assessed the effect of bacteriostatic treatment before or after bactericidal challenge on cell survival (Fig. 2 *A* and *B*). Rif did not kill *E. coli* up to 80× MIC (Fig. S2) but did cause robust killing in *S. aureus* with time-dependent kinetics, as opposed to respiration-enhancing antibiotics (Fig. S2).

In *E. coli*, all bacteriostatic antibiotics potently inhibited cell killing by several orders of magnitude, when applied before bactericidal antibiotics (Fig. 2 *B* and *C* and Fig. S3), and rapidly attenuated killing by bactericidal antibiotics when delivered after 30 min of initial bactericidal exposure (Fig. 2 *B* and *C* and Fig. S3). No combination of bacteriostatic antibiotics showed killing with Rif in *E. coli* (Fig. 2*C* and Fig. S3). Similarly, in *S. aureus* we observed broad and potent protection by preincubation with any bacteriostatic antibiotic before bactericidal challenge (Fig. 2*D* and Fig. S3). Bacteriostatic pretreatment of cells did not offer complete protection from Dapto challenge, consistent with its known effect on membrane integrity and charge-based mode of action (38). We again observed rapid interruption of cell killing after initial bactericidal treatment with any bacteriostatic drug (Fig. 2*D* and Fig. S3). We observed no impact of any bacteriostatic antibiotic on cell killing by Rif (Fig. 2*D* and Fig. S3). Taken together, this screen demonstrates that bacteriostatic translation inhibitors generally inhibit killing caused by a wide range of bactericidal antibiotics with differing cellular targets. The most notable exception was Rif in our *S. aureus* model, where lethality was not sensitive to bacteriostatic antibiotic cotreatment.

Due to the respiration-decelerating phenotype of Rif, we hypothesized that Rif-mediated killing would be antagonistic to

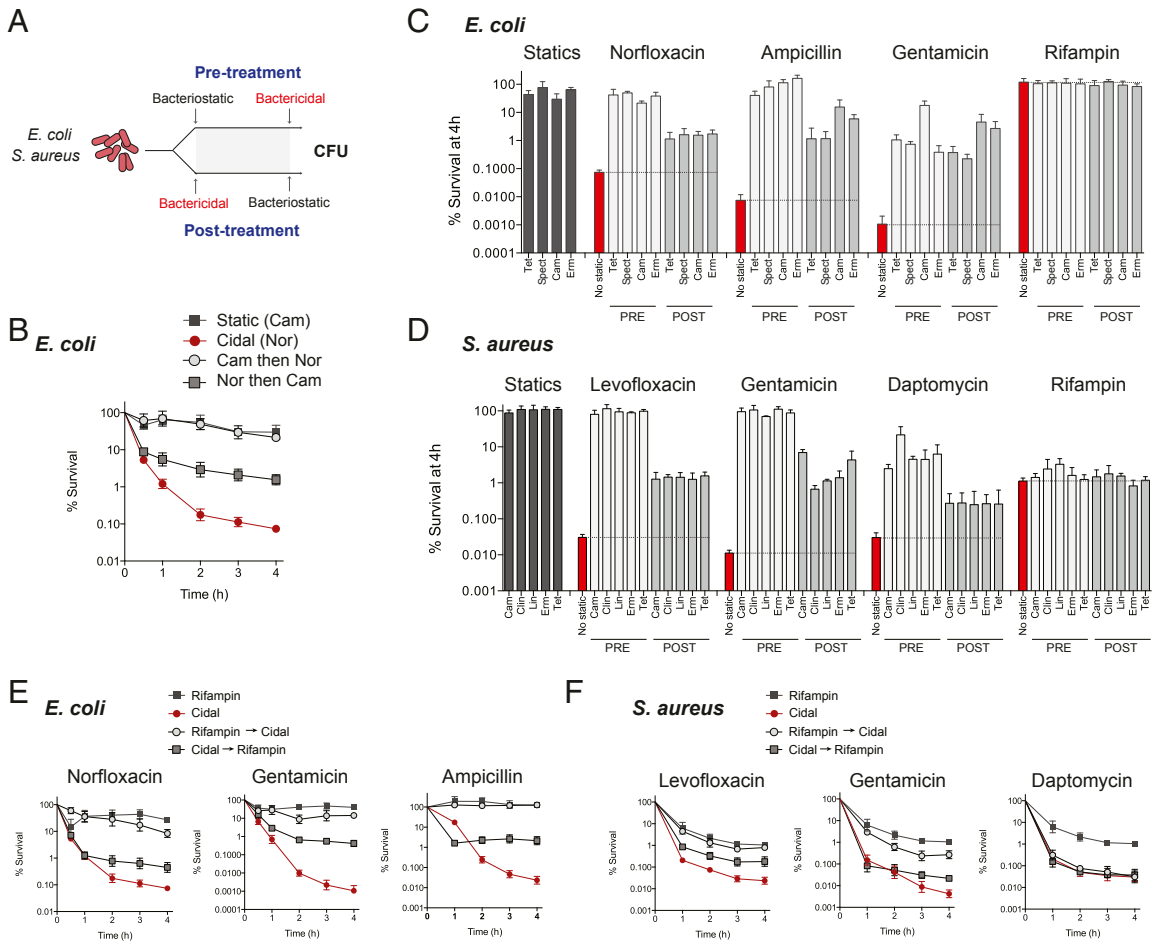

Fig. 2. Bacteriostatic antibiotics disrupt bactericidal lethality. (*A*) Time-kill analysis was performed on *E. coli* or *S. aureus* with bacteriostatic-bactericidal antibiotic pairs. Pretreatment: Bacteria were initially treated with bacteriostatic antibiotics (5× MIC) and subsequently challenged with bactericidal drugs. Posttreatment: Bacteria received initial bactericidal challenge, and bacteriostatic drugs were added second. (*B*) Representative time-kill analysis of norfloxacin and chloramphenicol combination. In all screens, combination therapy was compared against monotherapy with the single bacteriostatic and bactericidal antibiotic. Survivorship was assessed hourly. Screening of 36 individual antibiotic combinations in *E. coli* (*C*) and *S. aureus* (*D*). For both datasets, cell survival was plotted at the 4-h time point as log-change in colony-forming units per milliliter, expressed as percent survival relative to the population at $t = 0$. Bacteriostatic antibiotic monotherapy (black) is listed first. Bactericidal monotherapy (red) is followed by pretreatment (white) and posttreatment approaches (light gray). Chloramphenicol (Cam); clindamycin (Clin); erythromycin (Erm); linezolid (Lin); spectinomycin (Spect); Tetracycline (Tet). Error bars represent SEM of three independent experiments. (*E*) Time-kill curves of *E. coli* treated with norfloxacin, ampicillin, gentamicin, or rifampin monotherapy, compared with pretreatment or posttreatment with rifampin. (*F*) Time-kill curves of *S. aureus* treated with levofloxacin, gentamicin, daptomycin, or rifampin with rifampin pre- or posttreatment. Curves show mean ± SEM of three independent experiments.

respiration accelerators. Consistent with this proposal, we observed potent protection of *E. coli* by Rif from killing by Nor, Amp, and Gent, and rapid arrest in killing when Rif was added after bactericidal challenge (Fig. 2*E*), similar to bacteriostatic translation inhibitors. Rif is bactericidal in *S. aureus*; however, due to its time-dependent killing, we could compare Rif killing in combination with concentrations of Levo, Gent, and Dapto that produced more killing by at least an order of magnitude. In combination, we observed that Rif protected against the additional lethality induced by Levo or Gent (Fig. 2*F*). We did not observe any protection against killing by Dapto, consistent with the lack of respiration acceleration observed for this drug. Thus, Rif, which induces bacteriostatic-like respiratory changes, inhibits the lethality of respiration-accelerating bactericidal antibiotics similar to other bacteriostatic drugs.

Bacteriostatic Alterations to the Metabolome Correspond to Respiratory Deceleration. Given the divergent effects of bacteriostatic and bactericidal antibiotics on cellular respiration, we sought to characterize antibiotic-induced metabolic changes more broadly. In particular, we were interested in the dominant effect of respiration-decelerating antibiotics and whether this phenotype was derived from the general metabolic state of the cell. We profiled the metabolome of *S. aureus* treated with the respiration-decelerating antibiotics Cam, Lin, and Rif. We compared untreated cells at time 0 (UT0) with either a growth control (UT30) or cells exposed to antibiotic for 30 min. Our analysis yielded 353 robustly identified metabolites comprising eight superpathways and 63 subpathways (Fig. S4).

Hierarchical clustering of the metabolomics data identified broad trends across treatment conditions (Fig. 3*A*). We observed a marked progression of metabolism in the untreated sample between the 0-min and 30-min time points (Fig. 3*A*), reflecting growth during exponential phase. Treatment with the translation inhibitors Cam and Lin yielded indistinguishable metabolic profiles, characterized by elevation in two clusters of metabolites. The first group aligns with elevated metabolites in the UT0 sample and is enriched for amino acids ($P = 2.16 \times 10^{-9}$, hypergeometric test), suggesting an arrest in metabolic progression for these target-specific compounds. The second cluster is enriched for lipids ($P = 1.66 \times 10^{-9}$, hypergeometric test) and shows higher concentrations than either the UT0 or UT30 samples. Rif elicited a unique metabolic response, sharing some aspects of the translation inhibitors, but others that were unique (Fig. 3*A*).

We noted accumulation of ATP, ADP, and AMP specifically in response to respiration-decelerating antibiotics, consistent with decreased ATP utilization (Fig. 3*B* and Fig. S5), as well as a significant elevation in NADH, with more modest elevation in NAD+, suggesting a lowered redox state (Fig. 3*B*). We observed significant elevations in metabolites from central carbon metabolism (Fig. 3*C*, *Lower Left*), which, coupled to the energy state of the cell, suggested decreased metabolic rates. Further exploration of the metabolomics profiles revealed a striking accumulation of metabolites involved in transcription and translation, the specific targets of the drugs queried (Fig. 3*C*). Cam and Lin treatment resulted in marked accumulation of amino acids and amino acid precursors, indicative of decreased flux into polypeptide production (Fig. 3*C*, *Upper Left*). Similarly, Rif induced substantial increases in nucleotide and nucleotide precursors, consistent with inhibition of RNA production (Fig. 3*C*, *Upper Right*). Interestingly, Rif treatment also induced substantial accumulation of amino acid precursors whereas the translation inhibitors caused accumulation of nucleotides, consistent with the secondary arrest in cell turnover and DNA replication induced by these drugs. All three antibiotics resulted in significant accumulation of lipid and lipid precursors (Fig. 3*C*, *Lower Right*), which may be due to reduced utilization as an energy source or decreased cell turnover. Taken together, the metabolomics data indicate that inhibition of either transcription or translation results in the accumulation of energy currency and central metabolites coupled to a lower redox state, suggesting the association of reduced rates of respiration with lower overall metabolic rates, which derive from the arrest of a major macromolecular synthetic process.

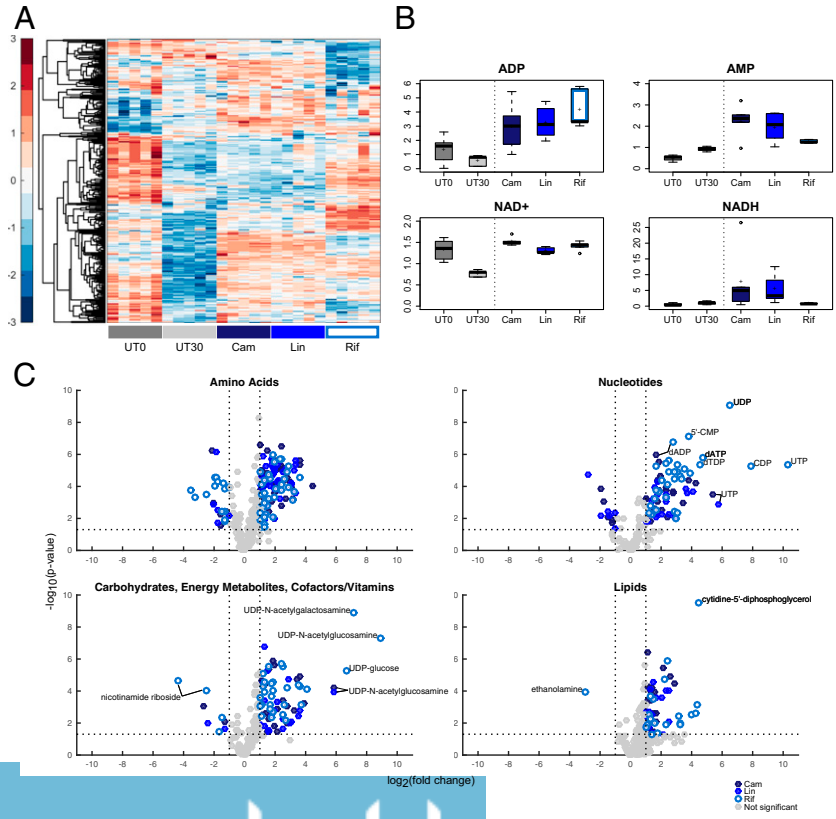

Fig. 3. Broad metabolite accumulation observed in bacteriostatic-treated *S. aureus*. In *A*, *B*, and *C*, UT0 represents metabolite levels at the time of antibiotic addition; UT30 represents 30 min of growth in the absence of antibiotics. Cam, Lin, and Rif treatments were assessed 30 min after exposure. (*A*) Hierarchical clustering of log-transformed and autoscaled relative metabolite concentrations for *S. aureus* treated with bacteriostatic antibiotics or vehicle. Five independent experiments are shown as replicates. (*B*) Box plots of relative concentration values from five independent experiments for ADP, AMP, NAD^+, and NADH. (*C*) Volcano plots showing the fold change (*x* axis) and significance (*y* axis) of metabolites detected in the major metabolic pathways. Blue shapes represent metabolites having a fold-change greater than two and *P* value less than 0.05; gray shapes represent metabolites that are not significantly changing. Fold changes are relative to UT30 control and are based on mean values of five independent experiments.

Attenuated Respiration Is Associated with Killing Arrest. Because bacteriostatic and bactericidal antibiotics stimulate competing effects on cellular respiration, we assessed the respiratory outcome of exposure to antibiotics in combination. We measured OCR of *E. coli* treated with the bacteriostatic antibiotic Cam 30 min before the addition of bactericidal antibiotics (Nor, Amp, Gent) (Fig. 4*A*). Treatment of cells in series was compared with cells given Cam alone, bactericidal antibiotic alone, or no antibiotic. Cells pretreated with Cam (asterisk) before bactericidal challenge (arrowhead) showed no detectable acceleration in cellular respiration after the addition of the bactericidal drug (Fig. 4*A*). Similarly, Cam addition after initial bactericidal treatment (arrowhead) resulted in immediate and potent suppression of OCR (Fig. 4*B*). Similar effects were observed for *S. aureus* (Fig. S6*A*). We asked whether prolonged treatment with bactericidal antibiotics would negate the effect of bacteriostatic suppression. *E. coli* were treated with Nor to initialize cell killing, followed by Cam at 30 or 60 min later. Even at 60 min, Cam addition rapidly attenuated cellular respiration and cell death (Fig. 4*C*). Similar results were obtained for Amp (Fig. S6*B*). Independent of the timing of addition, deceleration of cellular respiration driven by the bacteriostatic antibiotic was the dominant phenotype in combination treatment, consistent with the time–kill effect.

Accelerating Basal Respiration Potentiates Bactericidal Killing. The metabolomics data suggested that bacteriostatic inhibition of cellular respiration may be a byproduct of translation inhibition. Inhibition of translation may have additional nonmetabolic effects on the cell that could be the source of attenuated bactericidal activity. To assess whether cellular respiration itself was an important factor in bactericidal activity, we assessed cell killing in a genetic mutant lacking the three major cytochrome oxidases (Δ*cyoA* Δ*cydB* Δ*appB*). This mutant has previously been reported to have reduced rates of cellular respiration (39), which we confirmed in our assay (Fig. 5*A*). Treatment of cytochrome oxidase null bacteria with norfloxacin resulted in no appreciable acceleration of respiration (Fig. 5*A*, *Right*). When we assessed killing by bactericidal antibiotics, we found that the cytochrome oxidase null mutant was highly protected from the lethal effects of Nor, Amp, and Gent (Fig. 5*B*). Protection from Gent killing is likely related to the breakdown in proton motive force, leading to reduced drug uptake. In addition, consistent with previous results (39), we observed a reduced growth rate of the cytochrome oxidase null mutant relative to the WT, which may have affected its susceptibility to ampicillin.

We further hypothesized that accelerated basal respiration may potentiate killing by bactericidal antibiotics. We sought to uncouple electron transport from ATP production in *E. coli*. The known inhibitors of the F_1F_0 ATPase, oligomycin and venturicidin, do not have activity in *E. coli* whole-cell assays (40). Lacking a chemical approach, we used a knockout of the catalytic domain of the F_1F_0 ATPase (Δ*atpA*), which is a nonessential gene given the capacity for fermentative growth. Prior in silico models have predicted an elevated redox state in this mutant (41). We found that the Δ*atpA* mutant grew at the same rate as WT *E. coli* but reached stationary phase faster, potentially consistent with reduced efficiency of carbon utilization (Fig. 5*C* and Fig. S7*A*). Measurement of the extracellular acidification rate (ECAR) of this strain further confirmed a substantially higher rate of acid secretion, as expected in fermentative growth (Fig. 5*E*). Interestingly, we observed threefold elevations in basal OCR in this strain, indicating uncoupling of respiration from ATP production and a compensatory rise in respiration (Fig. 5*D*). We confirmed that these optical density-matched OCR variations were not due to differences in growth rate, to total cell numbers plated, or to the density of cells in the experiment (Fig. S7).

Treatment of the Δ*atpA* strain with Amp and Nor resulted in substantially increased killing (Fig. 5*F*). We found a leftward shift in the gentamicin minimum bactericidal concentration (MBC) curve, consistent with a likely increase in drug uptake due to elevated proton motive force from altered respiration (Fig. 5*F*). We were further interested in how bacteriostatic antibiotic treatment may protect against killing in the context of an accelerated basal respiration state. In time–kill analysis, the Δ*atpA* mutant exhibited approximately two orders of magnitude of increased killing relative to WT (Fig. 5*G*). Pretreatment with Cam for 30 min, followed by Nor challenge, led to breakthrough killing in the Δ*atpA* mutant (Fig. 5*H*). Interestingly, Cam treatment of the Δ*atpA* mutant decelerates OCR, but with high levels of residual respiration present in this mutant relative to the WT (Fig. 5*I*). Thus, elevated basal respiration increases killing by respiration-accelerating bactericidal antibiotics.

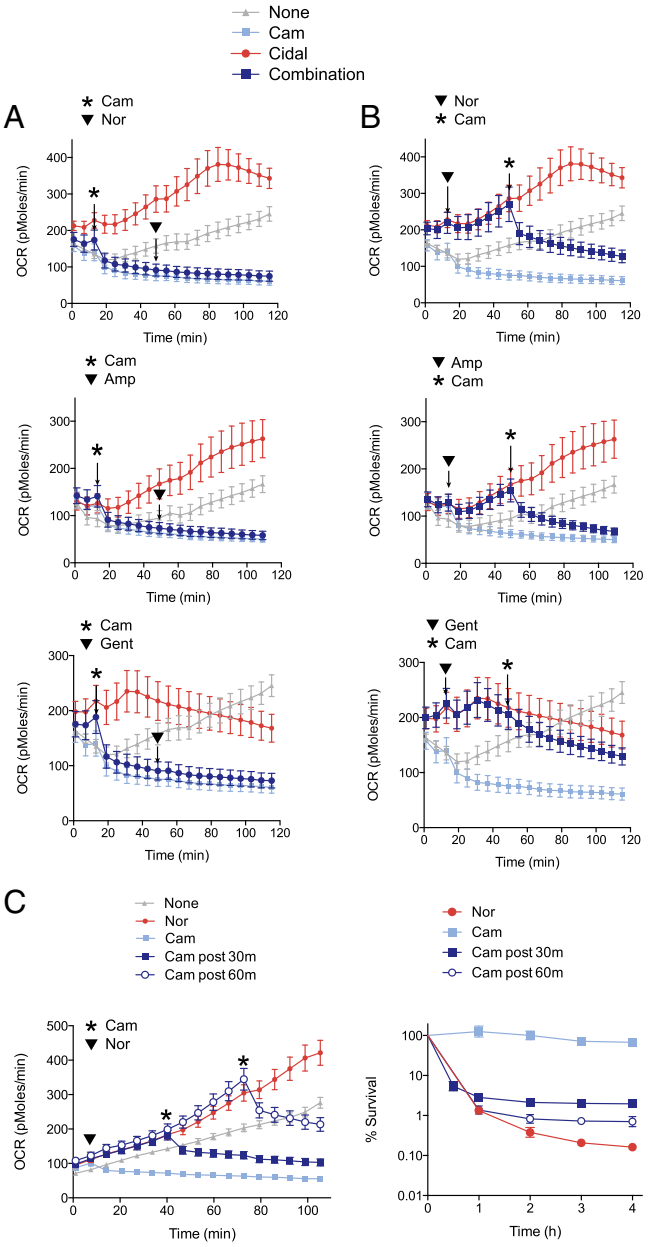

Fig. 4. Bacteriostatic antibiotics dominantly inhibit bactericidal respiratory activity. (*A*) *E. coli* was pretreated with the bacteriostatic antibiotic chloramphenicol (Cam, asterisk) for 30 min, then challenged with bactericidal antibiotics (arrowhead). (*B*) OCR versus time of *E. coli* treated with bactericidal antibiotic first (arrowhead), and then Cam after 30 min (asterisk). Respiration rates were compared with untreated cells, Cam treatment alone, or bactericidal antibiotic treatment alone. (*C*) OCR of *E. coli* treated with Nor at 5× MIC (arrowhead), and then treated with Cam at 30 min or 60 min (asterisks). (*Right*) Inhibition of Nor killing in *E. coli* after addition of Cam at 30 or 60 min.

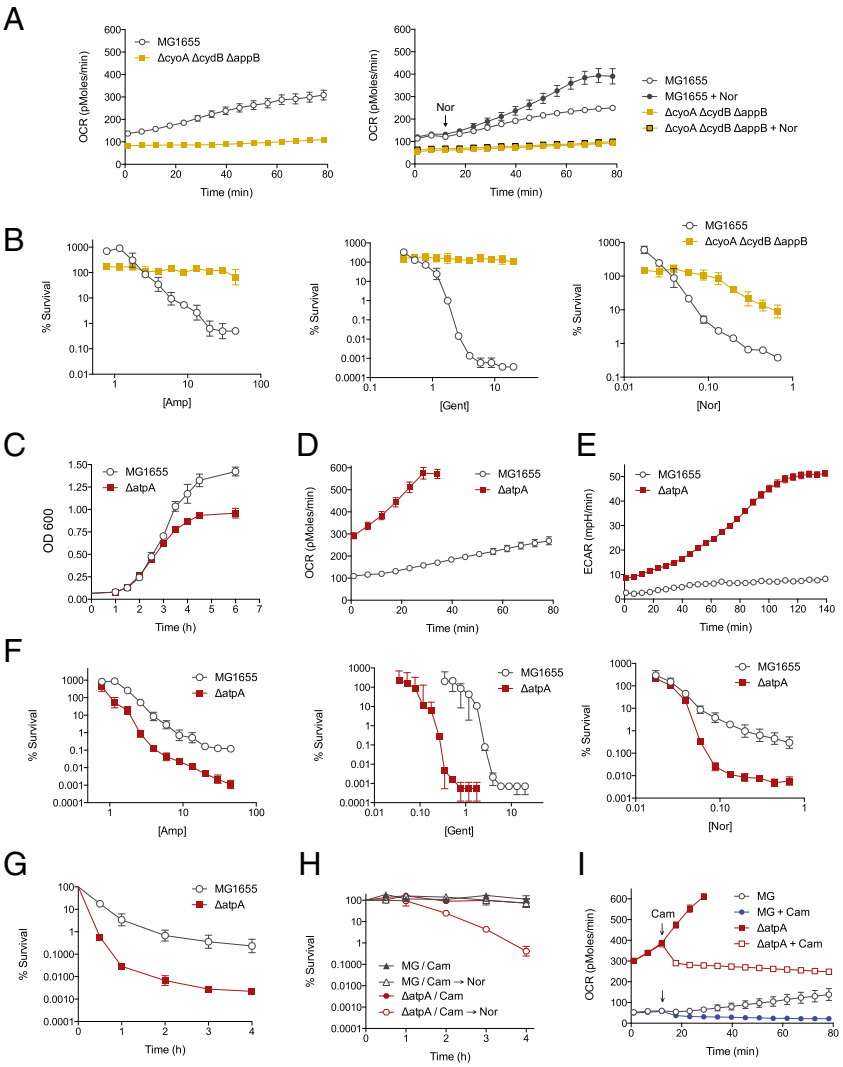

Fig. 5. Uncoupling of respiration enhances bactericidal killing. (*A*) Basal cellular respiration of Δ*cyoA* Δ*cydB* Δ*appB* was compared with WT MG1655 using optical density-matched inputs. (*Right*) OCR response to challenge with Nor (250 ng/mL). (*B*) Cell survival as a function of antibiotic concentration after 90 min of drug exposure for Amp, Gent, and Nor. (*C*) Optical density of MG1655 or Δ*atpA* in M9 at 600 nanometers. (*D*) Basal oxygen consumption rate of optical density-matched cells. (*E*) Basal extracellular acidification rate (ECAR) in milli-pH/min of optical density-matched cells. (*F*) Cell survival as a function of antibiotic concentration after 90 min of drug exposure for Amp, Gent, and Nor. (*G*) Time-kill kinetics of MG1655 compared with Δ*atpA* with Nor (250 ng/mL). (*H*) Time-kill kinetics of cells preincubated with Cam (50 μg/mL) for 30 min before Nor (250 ng/mL) challenge. (*I*) Oxygen consumption perturbation induced by addition of Cam (50 μg/mL) in MG1655 and Δ*atpA*.

Discussion

A key concept supported by this work is that inhibition of antibiotic targets results in downstream metabolic perturbations. The direction of the shift, however, seems to depend upon the function of the target that is inhibited and is linked to the bacteriostatic or bactericidal outcome. Inhibition of macromolecular synthesis (i.e., transcription or translation) was associated with decreased bacterial cellular respiration. Interestingly, the majority of bacteriostatic antibiotics inhibit protein production (42), which as a process is the largest single consumer of total metabolic output (23, 43). We observed a marked accumulation of amino acids and nucleotides in response to translation and transcription inhibitors, respectively, reflective of reduced incorporation into peptide or RNA chains. In addition, we observed accumulation of amino acid and nucleotide precursors, indicative of bottlenecking of flux from these pools as a direct result of bacteriostatic antibiotic activity. This effect on amino acid and nucleotide metabolism was associated with the accumulation of central carbon metabolites, the flow of which powers the electron transport chain. Prior metabolomic and proteomic analyses of bacteriostatic antibiotic treatments have suggested that central metabolism is suppressed in response to bacteriostatic antibiotic treatment (26, 44). Our data further support this model, suggesting that inhibition of these core cellular processes may reduce energy demand and secondarily suppress rates of cellular respiration and ATP production (25).

On the other hand, most canonical bactericidal antibiotics were associated with accelerated respiratory activity in our study and others (35). It has been hypothesized that bactericidal antibiotics lead to metabolic instability and the formation of toxic ROS as part of their lethality (28, 29, 35, 36). Acceleration of cellular respiration by bactericidal antibiotics may be a potential source of ROS (45). Our work supports this model by showing that tuning rates of basal cellular respiration can significantly impact bactericidal efficacy. What remains unclear is how bactericidal antibiotic target inhibition may lead to acceleration of cellular respiration. Because bacteriostatic antibiotics arrest a metabolically costly process and reduce ATP demand, it is possible that bactericidal antibiotics may aberrantly increase metabolic demand by virtue of their drug–target interaction. In support of this notion, a recent study on the β-lactam mechanism of action revealed that these drugs cause the formation of a futile cycle in the production and degradation of peptidoglycan (46). The formation of a macromolecular futile cycle may accelerate cellular respiration to meet the metabolic demand of dead-end peptidoglycan synthesis. Identification of the mechanism by which β-lactams, quinolones, aminoglycosides, and other bactericidal antibiotics accelerate respiration requires further study.

Under aerobic conditions, *E. coli* uses a branched electron transport chain composed of two NADH-quinone oxidoreductases and three quinol oxidases that efficiently couple electron exchange to ATP production by the F_1F_0 ATPase (37, 47). Manipulation of the rate of cellular respiration directly by gene knockout resulted in

significant perturbations in bactericidal killing, suggesting a specific role for respiration in antibiotic lethality. Interestingly, several promising antibiotic leads have recently been characterized that target energy production by inhibiting components of the electron transport chain directly (48, 49). The F_1F_0 ATPase is the target of bedaquiline, a novel antibiotic for the treatment of tuberculosis (50, 51). The mechanism of action has been thought to be due to depletion of available energy currency (52); however, more recent analysis has revealed that it uncouples cellular respiration from ATP synthesis, resulting in a futile proton cycle that is linked to cell death (53). The degree of respiratory acceleration caused by knockout of the F_1F_0 catalytic domain in *E. coli* in our study (Fig. 5) was very similar to that produced by chemical inhibition by bedaquiline, suggesting that inhibition of catalysis by the ATPase may be a general strategy to induce metabolic dysfunction in bacteria. Interestingly, inhibition of the F_1F_0 ATPase has been shown to lead to increased ROS production in eukaryotes (54) and could potentially lead to a similar outcome in bacteria. Our data suggest that chemically targeting the bacterial F_1F_0 ATPase could serve as means to boost the activity of bactericidal antibiotics and represents an intriguing target for antibiotic adjuvant therapy.

Antibiotics are effective because they inhibit critical functional components of bacterial cellular architecture. The concept of a "bacteriostatic" or "bactericidal" antibiotic has largely rested on phenomenological changes in cell state. Our data extend these concepts by demonstrating that these phenotypic outcomes are, in part, a direct reflection of the metabolic perturbation induced by target inhibition. We showed that growth inhibition associated with bacteriostatic antibiotics is linked to suppression of cellular respiration and broader metabolism. Cell death from bactericidal antibiotics, on the other hand, drives acceleration of respiration, and perturbation of the basal level of metabolism significantly impacts the efficacy of bactericidal therapy. Overall, our data support the hypothesis that antibiotics alter the metabolic state of bacteria, contributing to the resulting lethality, stasis, or tolerance, and, further, that the existing metabolic environment of bacteria influences their susceptibility to antibiotics.

Methods

Strains, Media, and Growth Conditions. *E. coli* K12 strain MG1655 and *S. aureus* strain ATCC 25923 were used in this study. The *E. coli* Δ*atpA* and Δ*cyoA* Δ*cydB* Δ*appB* mutants were constructed by P1 transduction from the Keio collection. *E. coli* was cultured in M9 minimal media (Fisher), supplemented with 0.2% casamino acids and 10 mM glucose. *S. aureus* was cultured in tryptic soy broth (TSB) (Teknova). Cells were grown at 37 °C on a rotating shaker at 300 rpm in flasks or at 900 rpm in plate shakers.

Antibiotics and Chemicals. *E. coli* cells were treated with bactericidal antibiotics at 5× minimum inhibitory concentration (MIC) (by macrobroth dilution): ampicillin (Amp) 10 $\mu g \cdot mL^{-1}$, norfloxacin (Nor) 250 $ng \cdot mL^{-1}$, gentamicin (Gent) 5 $\mu g \cdot mL^{-1}$. Rifampin (Rif) was used at 5× MIC (250 $\mu g \cdot mL^{-1}$) for consistency, despite the absence of detectable bactericidal activity. Bacteriostatic antibiotics were used in the screen at 5× MIC unless otherwise indicated: chloramphenicol (Cam) 50 $\mu g \cdot mL^{-1}$, erythromycin (Erm) 500 $\mu g \cdot mL^{-1}$, spectinomycin (Spect) 200 $\mu g \cdot mL^{-1}$, tetracycline (Tet) 10 $\mu g \cdot mL^{-1}$. For *S. aureus*, bactericidal antibiotics were used at 10× MIC to generate biological equivalents of cell killing, unless otherwise indicated: levofloxacin (Levo) 2 $\mu g \cdot mL^{-1}$, Gent 5 $\mu g \cdot mL^{-1}$, daptomycin (Dapto) 16 $\mu g \cdot mL^{-1}$, rifampin (Rif) 125 $ng \cdot mL^{-1}$. Daptomycin treatments included 50 $\mu g \cdot mL^{-1}$ calcium chloride, as previously reported, for activity (55). Bacteriostatic antibiotics were used, unless otherwise indicated, at 5× MIC: Cam 50 $\mu g \cdot mL^{-1}$, linezolid (Lin) 25 $\mu g \cdot mL^{-1}$, clindamycin (Clin) 1 $\mu g \cdot mL^{-1}$, Erm 5 $\mu g \cdot mL^{-1}$, Tet 2 $\mu g \cdot mL^{-1}$. All antibiotics were purchased from Sigma.

Bacterial Respiration. The XF^{e}96 Extracellular Flux Analyzer (Seahorse Bioscience) was used to quantitate oxygen consumption rates (OCRs) (35) and extracellular acidification rates (ECARs). An overnight of MG1655 *E. coli* cells was diluted 1:200 into fresh M9 media and grown to an OD_{600} of ∼0.3. Cells were diluted to 2× the final OD, and 90 μL of diluted cells was added to XF Cell Culture Microplates precoated with poly-D-lysine (PDL) (35). Cells were centrifuged for 10 min at 1,400 × *g* in a Heraeus Multifuge ×1R (M-20 rotor) to attach them to the precoated plates. After centrifugation, 90 μL of fresh M9 media was added to each well. To assure uniform cellular seeding, initial OCR was measured for two cycles (7 min) before the injection of antibiotics. *S. aureus* OCR experiments were run in a similar manner, with the exception that the cells were diluted into TSB after the initial LB overnight, and the OCR measurements were similarly run in TSB. Maximal OCR read on the SeaHorse is ∼700–800 pmol/min, after which point the consumption rate exceeds the replenishment of the system and curves show a false declination in OCR, which have been excluded from graphical presentation.

OCR from *S. aureus* grown in TSB was normalized to the number of viable cells quantitated using the LIVE/DEAD BacLight Bacterial Viability and Counting Kit-for Flow Cytometry (Life Technologies), according to kit instructions. For this assay, cells were cultured and treated on a parallel XF Cell Culture Microplate and assayed at 30 min after the addition of antibiotics. To prepare cells for measurement, 50 μL of cell culture was added to a 250-μL assay mix [20 μL of fluorescent beads, 10 μL of SYBR green DNA stain, and 20 μL of propidium iodide in a 10-mL assay medium (150 mM NaCl)] and incubated for 15 min before counting. Measurements were made with a FACS Aria II flow cytometer (Becton Dickinson). The following photomultiplier tube voltages were used: forward scatter (FSC) 200, side scatter 200, fluorescence signal 1A 325, fluorescence signal 2A 390. Acquisition was performed at a low flow rate (∼30 events per s), with thresholding on FSC at a value of 1,000.

Time-Kill and MBC Analyses. For time-kill analysis, overnight samples of *E. coli* or *S. aureus* were diluted 1:200 into 25 mL of fresh media and grown in a 250-mL baffled flask to an OD_{600} of ∼0.2–0.3. Cells were then plated in a six-well dish, and antibiotics were added at the appropriate concentration. At specified time points (30 min for *E. coli*, and 15 min for *S. aureus*), a second antibiotic or vehicle control was added to wells if indicated. The difference in time of addition was related to the rate of growth in defined media (*E. coli*) versus rich media (*S. aureus*). Aliquots of 300 μL were taken at specified times, serially diluted, and spot-plated onto LB agar plates to determine colony-forming units per mL ($cfu \cdot mL^{-1}$). Dilutions that grew 10–50 colonies were counted. Percent survival was determined by dividing the $cfu \cdot mL^{-1}$ of a sample at each time point by the initial $cfu \cdot mL^{-1}$ of that sample.

Minimum bactericidal concentration (MBC) curves were performed on MG1655, Δ*cyoA* Δ*cydB* Δ*appB*, or the Δ*atpA* mutant. Overnight cultures were diluted 1:200 in M9 medium and grown to OD 0.2. Cells were exposed to antibiotics at 1.5-fold dilutions for 90 min, and cfu analysis was performed.

Metabolic Profiling. *S. aureus* was grown in 100 mL of TSB in 1-L baffled flasks to an OD_{600} of ∼0.2–0.3. Control cells were either collected at this time point (UT0), or cells were treated with antibiotics or vehicle. Antibiotics were added for 30 min: linezolid (Lin, 20 $\mu g \cdot mL^{-1}$), chloramphenicol (Cam, 50 $\mu g \cdot mL^{-1}$), and rifampin (Rif, 32 $ng \cdot mL^{-1}$) were all used at 4× MIC. Quintuplicate samples were collected by centrifugation at 1,400 × *g* × 5 min at 4 °C, washed once in ice cold PBS, and snap frozen in liquid nitrogen before metabolomic analysis. Cells were lysed and assayed by Metabolon Inc. as previously described (56).

Relative concentration data for each detected metabolite were normalized by BRADFORD protein concentration and scaled such that the median value across all samples was equal to one. Only robustly identified metabolites, defined as metabolites being identified in at least three out of five of the replicates across all conditions, were retained for analysis. All analyses were then performed in Matlab. The k-nearest neighbors approach, with the standardized Euclidean distance metric, was used to impute remaining missing data. A Welch's two-sample *t* test was performed on log-transformed data to evaluate significant changes in metabolite abundance between conditions, and the mafdr Matlab function was used to correct for multiple hypothesis testing. Hierarchical clustering (correlation and average were used as the distance and linkage metrics, respectively) and principal component analysis were performed on log-transformed and autoscaled metabolite data. Box plots were constructed in R using normalized relative concentration data. To determine pathway enrichment, the hygecdf function was used to perform a hypergeometric test in Matlab. ATP concentrations, which were not detected on the Metabolon platform, were determined using a bioluminescent assay (Sigma), with ATP concentration corrected by total protein as determined by BCA assay (Pierce).

ACKNOWLEDGMENTS. This work was supported by the Howard Hughes Medical Institute (J.J.C.), National Institutes of Health Director's Pioneer Award DP1 OD003644 (to J.J.C.), and a Merieux Research Grant from the Institut Merieux (to A.S.K. and J.J.C.). M.A.L. is supported in part by the Clinical Fellows program from the Wyss Institute at Harvard University.

1. Pankey GA, Sabath LD (2004) Clinical relevance of bacteriostatic versus bactericidal mechanisms of action in the treatment of Gram-positive bacterial infections. *Clin Infect Dis* 38(6):864–870.
2. Finberg RW, et al. (2004) The importance of bactericidal drugs: Future directions in infectious disease. *Clin Infect Dis* 39(9):1314–1320.
3. Chowdhury MH, Tunkel AR (2000) Antibacterial agents in infections of the central nervous system. *Infect Dis Clin North Am* 14(2):391–408.
4. Archer G, Fekety FR, Jr (1977) Experimental endocarditis due to Pseudomonas aeruginosa. II. Therapy with carbenicillin and gentamicin. *J Infect Dis* 136(3): 327–335.
5. Carrizosa J, Kaye D (1977) Antibiotic concentrations in serum, serum bactericidal activity, and results of therapy of streptococcal endocarditis in rabbits. *Antimicrob Agents Chemother* 12(4):479–483.
6. Weinstein MP, et al. (1985) Multicenter collaborative evaluation of a standardized serum bactericidal test as a prognostic indicator in infective endocarditis. *Am J Med* 78(2):262–269.
7. Weinstein MP, Stratton CW, Hawley HB, Ackley A, Reller LB (1987) Multicenter collaborative evaluation of a standardized serum bactericidal test as a predictor of therapeutic efficacy in acute and chronic osteomyelitis. *Am J Med* 83(2):218–222.
8. Klastersky J (1986) Concept of empiric therapy with antibiotic combinations: Indications and limits. *Am J Med* 80(5C):2–12.
9. Ankomah P, Levin BR (2012) Two-drug antimicrobial chemotherapy: A mathematical model and experiments with Mycobacterium marinum. *PLoS Pathog* 8(1):e1002487.
10. Ankomah P, Johnson PJ, Levin BR (2013) The pharmaco -, population and evolutionary dynamics of multi-drug therapy: Experiments with S. aureus and E. coli and computer simulations. *PLoS Pathog* 9(4):e1003300.
11. Crumplin GC, Smith JT (1975) Nalidixic acid: An antibacterial paradox. *Antimicrob Agents Chemother* 8(3):251–261.
12. Deitz WH, Cook TM, Goss WA (1966) Mechanism of action of nalidixic acid on Escherichia coli. 3. Conditions required for lethality. *J Bacteriol* 91(2):768–773.
13. Winslow DL, Damme J, Dieckman E (1983) Delayed bactericidal activity of beta-lactam antibiotics against Listeria monocytogenes: antagonism of chloramphenicol and rifampin. *Antimicrob Agents Chemother* 23(4):555–558.
14. Watanakunakorn C, Guerriero JC (1981) Interaction between vancomycin and rifampin against Staphylococcus aureus. *Antimicrob Agents Chemother* 19(6):1089–1091.
15. Johansen HK, Jensen TG, Dessau RB, Lundgren B, Frimodt-Moller N (2000) Antagonism between penicillin and erythromycin against Streptococcus pneumoniae in vitro and in vivo. *J Antimicrob Chemother* 46(6):973–980.
16. Weeks JL, Mason EO, Jr, Baker CJ (1981) Antagonism of ampicillin and chloramphenicol for meningeal isolates of group B streptococci. *Antimicrob Agents Chemother* 20(3):281–285.
17. Rocco V, Overturf G (1982) Chloramphenicol inhibition of the bactericidal effect of ampicillin against Haemophilus influenzae. *Antimicrob Agents Chemother* 21(2): 349–351.
18. Brown TH, Alford RH (1984) Antagonism by chloramphenicol of broad-spectrum beta-lactam antibiotics against Klebsiella pneumoniae. *Antimicrob Agents Chemother* 25(4):405–407.
19. Lepper MH, Dowling HF (1951) Treatment of pneumococcic meningitis with penicillin compared with penicillin plus aureomycin: Studies including observations on an apparent antagonism between penicillin and aureomycin. *AMA Arch Intern Med* 88(4): 489–494.
20. Mathies AW, Jr, Leedom JM, Ivler D, Wehrle PF, Portnoy B (1967) Antibiotic antagonism in bacterial meningitis. *Antimicrob Agents Chemother (Bethesda)* 7:218–224.
21. Coyle EA, Cha R, Rybak MJ (2003) Influences of linezolid, penicillin, and clindamycin, alone and in combination, on streptococcal pyrogenic exotoxin a release. *Antimicrob Agents Chemother* 47(5):1752–1755.
22. Stevens DL, et al. (2007) Impact of antibiotics on expression of virulence-associated exotoxin genes in methicillin-sensitive and methicillin-resistant Staphylococcus aureus. *J Infect Dis* 195(2):202–211.
23. Stouthamer AH (1973) A theoretical study on the amount of ATP required for synthesis of microbial cell material. *Antonie van Leeuwenhoek* 39(3):545–565.
24. Li GW, Burkhardt D, Gross C, Weissman JS (2014) Quantifying absolute protein synthesis rates reveals principles underlying allocation of cellular resources. *Cell* 157(3): 624–635.
25. Koebmann BJ, Westerhoff HV, Snoep JL, Nilsson D, Jensen PR (2002) The glycolytic flux in Escherichia coli is controlled by the demand for ATP. *J Bacteriol* 184(14): 3909–3916.
26. Lin X, Kang L, Li H, Peng X (2014) Fluctuation of multiple metabolic pathways is required for Escherichia coli in response to chlortetracycline stress. *Mol Biosyst* 10(4):901–908.
27. Rittershaus ES, Baek SH, Sassetti CM (2013) The normalcy of dormancy: Common themes in microbial quiescence. *Cell Host Microbe* 13(6):643–651.
28. Dwyer DJ, Kohanski MA, Hayete B, Collins JJ (2007) Gyrase inhibitors induce an oxidative damage cellular death pathway in Escherichia coli. *Mol Syst Biol* 3:91.
29. Kohanski MA, Dwyer DJ, Hayete B, Lawrence CA, Collins JJ (2007) A common mechanism of cellular death induced by bactericidal antibiotics. *Cell* 130(5): 797–810.
30. Kohanski MA, Dwyer DJ, Wierzbowski J, Cottarel G, Collins JJ (2008) Mistranslation of membrane proteins and two-component system activation trigger antibiotic-mediated cell death. *Cell* 135(4):679–690.
31. Nandakumar M, Nathan C, Rhee KY (2014) Isocitrate lyase mediates broad antibiotic tolerance in Mycobacterium tuberculosis. *Nat Commun* 5:4306.
32. Baek SH, Li AH, Sassetti CM (2011) Metabolic regulation of mycobacterial growth and antibiotic sensitivity. *PLoS Biol* 9(5):e1001065.
33. Thomas VC, et al. (2013) A dysfunctional tricarboxylic acid cycle enhances fitness of Staphylococcus epidermidis during β-lactam stress. *MBio* 4(4):e00437–13.
34. Grant SS, Kaufmann BB, Chand NS, Haseley N, Hung DT (2012) Eradication of bacterial persisters with antibiotic-generated hydroxyl radicals. *Proc Natl Acad Sci USA* 109(30): 12147–12152.
35. Dwyer DJ, et al. (2014) Antibiotics induce redox-related physiological alterations as part of their lethality. *Proc Natl Acad Sci USA* 111(20):E2100–E2109.
36. Foti JJ, Devadoss B, Winkler JA, Collins JJ, Walker GC (2012) Oxidation of the guanine nucleotide pool underlies cell death by bactericidal antibiotics. *Science* 336(6079): 315–319.
37. Bettenbrock K, et al. (2014) Towards a systems level understanding of the oxygen response of Escherichia coli. *Adv Microb Physiol* 64:65–114.
38. Silverman JA, Perlmutter NG, Shapiro HM (2003) Correlation of daptomycin bactericidal activity and membrane depolarization in Staphylococcus aureus. *Antimicrob Agents Chemother* 47(8):2538–2544.
39. Portnoy VA, Herrgård MJ, Palsson BO (2008) Aerobic fermentation of D-glucose by an evolved cytochrome oxidase-deficient Escherichia coli strain. *Appl Environ Microbiol* 74(24):7561–7569.
40. Perlin DS, Latchney LR, Senior AE (1985) Inhibition of Escherichia coli H+-ATPase by venturicidin, oligomycin and ossamycin. *Biochim Biophys Acta* 807(3):238–244.
41. Brynildsen MP, Winkler JA, Spina CS, MacDonald IC, Collins JJ (2013) Potentiating antibacterial activity by predictably enhancing endogenous microbial ROS production. *Nat Biotechnol* 31(2):160–165.
42. Wilson DN (2014) Ribosome-targeting antibiotics and mechanisms of bacterial resistance. *Nat Rev Microbiol* 12(1):35–48.
43. Schneider DA, Gaal T, Gourse RL (2002) NTP-sensing by rRNA promoters in Escherichia coli is direct. *Proc Natl Acad Sci USA* 99(13):8602–8607.
44. Zhang B, et al. (2011) NMR analysis of a stress response metabolic signaling network. *J Proteome Res* 10(8):3743–3754.
45. Wang JH, et al. (2014) Sigma S-dependent antioxidant defense protects stationary-phase Escherichia coli against the bactericidal antibiotic gentamicin. *Antimicrob Agents Chemother* 58(10):5964–5975.
46. Cho H, Uehara T, Bernhardt TG (2014) Beta-lactam antibiotics induce a lethal malfunctioning of the bacterial cell wall synthesis machinery. *Cell* 159(6):1300–1311.
47. Richardson DJ (2000) Bacterial respiration: A flexible process for a changing environment. *Microbiology* 146(Pt 3):551–571.
48. Rubin H, et al. (2015) Acinetobacter baumannii OxPhos inhibitors as selective anti-infective agents. *Bioorg Med Chem Lett* 25(2):378–383.
49. Schurig-Briccio LA, Yano T, Rubin H, Gennis RB (2014) Characterization of the type 2 NADH:menaquinone oxidoreductases from Staphylococcus aureus and the bactericidal action of phenothiazines. *Biochim Biophys Acta* 1837(7):954–963.
50. Andries K, et al. (2005) A diarylquinoline drug active on the ATP synthase of Mycobacterium tuberculosis. *Science* 307(5707):223–227.
51. Koul A, et al. (2007) Diarylquinolines target subunit c of mycobacterial ATP synthase. *Nat Chem Biol* 3(6):323–324.
52. Koul A, et al. (2014) Delayed bactericidal response of Mycobacterium tuberculosis to bedaquiline involves remodelling of bacterial metabolism. *Nat Commun* 5:3369.
53. Hards K, et al. (2015) Bactericidal mode of action of bedaquiline. *J Antimicrob Chemother*, 10.1093/jac/dkv054.
54. Formentini L, Sánchez-Aragó M, Sánchez-Cenizo L, Cuezva JM (2012) The mitochondrial ATPase inhibitory factor 1 triggers a ROS-mediated retrograde prosurvival and proliferative response. *Mol Cell* 45(6):731–742.
55. Eliopoulos GM, et al. (1986) In vitro and in vivo activity of LY 146032, a new cyclic lipopeptide antibiotic. *Antimicrob Agents Chemother* 30(4):532–535.
56. Shakoury-Elizeh M, et al. (2010) Metabolic response to iron deficiency in Saccharomyces cerevisiae. *J Biol Chem* 285(19):14823–14833.